Development 127, 801-812 (2000)
Printed in Great Britain © The Company of Biologists Limited 2000
DEV8690

Receptor tyrosine phosphatases regulate axon guidance across the midline of the *Drosophila* embryo

Qi Sun[1], Sami Bahri[2], Aloisia Schmid[3], William Chia[2] and Kai Zinn[1,*]

[1]Division of Biology, California Institute of Technology, Pasadena, CA 91125, USA
[2]Institute of Molecular and Cell Biology, National University of Singapore, Singapore 117609
[3]Institute of Neuroscience and Institute of Molecular Biology, University of Oregon, Eugene, OR 97403, USA
*Author for correspondence (e-mail: zinnk@its.caltech.edu)

Accepted 22 November 1999; published on WWW 26 January 2000

SUMMARY

Neural receptor-linked protein tyrosine phosphatases (RPTPs) are required for guidance of motoneuron and photoreceptor growth cones in *Drosophila.* These phosphatases have not been implicated in growth cone responses to specific guidance cues, however, so it is unknown which aspects of axonal pathfinding are controlled by their activities. Three RPTPs, known as DLAR, DPTP69D, and DPTP99A, have been genetically characterized thus far. Here we report the isolation of mutations in the fourth neural RPTP, DPTP10D. The analysis of double mutant phenotypes shows that DPTP10D and DPTP69D are necessary for repulsion of growth cones from the midline of the embryonic central nervous system. Repulsion is thought to be triggered by binding of the secreted protein Slit, which is expressed by midline glia, to Roundabout (Robo) receptors on growth cones. Robo repulsion is downregulated by the Commissureless (Comm) protein, allowing axons to cross the midline. Here we show that the *Rptp* mutations genetically interact with *robo*, *slit* and *comm*. The nature of these interactions suggests that DPTP10D and DPTP69D are positive regulators of Slit/Roundabout repulsive signaling. We also show that elimination of all four neural RPTPs converts most noncrossing longitudinal pathways into commissures that cross the midline, indicating that tyrosine phosphorylation controls the manner in which growth cones respond to midline signals.

Key words: Neural development, *Drosophila* Neurogenetics, Receptor tyrosine phosphatase, Tyrosine phosphorylation, Growth cone repulsion, Axon guidance, *roundabout, commissureless, Drosophila melanogaster*

INTRODUCTION

During embryonic development, growth cones, which form the leading edges of neuronal processes, sample the environment and make pathfinding decisions. Contacts between growth cone surface receptors and attractive or repulsive guidance cues on surrounding cells and in the extracellular matrix affect signal transduction cascades within the growth cones (Goodman, 1996). These signaling events change the growth cone's cytoskeleton, altering its morphology and direction of movement.

One signaling mechanism by which growth cones respond to guidance factors is the control of tyrosine phosphorylation. Phosphotyrosine in growth cones is generated by receptor tyrosine kinases that are activated by direct binding to extracellular ligands and by cytoplasmic tyrosine kinases which interact with a variety of surface receptors. Receptor-linked protein tyrosine phosphatases (RPTPs), which reverse the reactions catalyzed by tyrosine kinases, also regulate tyrosine phosphorylation within growth cones. The five known *Drosophila* RPTPs have receptor-like extracellular regions consisting of immunoglobulin-like and/or fibronectin type III domains, linked *via* a single transmembrane domain to a cytoplasmic region containing one or two phosphatase domains. Strikingly, four of these five RPTPs (DPTP10D, DLAR, DPTP69D and DPTP99A) are expressed only on central nervous system (CNS) axons in the embryo (reviewed by Desai et al., 1997b). RPTPs are also localized to axons and growth cones in vertebrate systems (reviewed by Stoker and Dutta, 1998).

Genetic studies in *Drosophila* have demonstrated that DLAR, DPTP69D and DPTP99A are important regulators of motor axon guidance decisions (Desai et al., 1996, 1997a; Krueger et al., 1996). DPTP69D is required for normal innervation of the lamina by photoreceptor growth cones (Garrity et al., 1999). However, we do not currently have a framework for understanding how RPTPs control growth cone pathfinding in the neuromuscular system or the larval optic lobes. This is because the ligands and substrates that interact with RPTPs in vivo are unknown, and the attractive and repulsive guidance cues that guide motoneuron and photoreceptor growth cones to their targets are not well defined.

In this paper, we link RPTPs to a specific pathfinding event by showing that two of these phosphatases regulate repulsion from the CNS midline. Axon guidance at the midline has been

intensively studied, and several of the key molecules controlling attractive and repulsive interactions between neuronal growth cones and the specialized midline glial cells have already been identified. Attractive signals emanating from the midline are required to recruit growth cones into commissural pathways that cross over to the contralateral side of the embryo. In *Drosophila*, these attractive factors include two Netrins, which are secreted proteins used in both vertebrates and invertebrates for control of guidance at the midline (Harris et al., 1996; Mitchell et al., 1996).

The midline also produces signals that repel growth cones. These are necessary to prevent longitudinal axons that express receptors for attractive factors from crossing the midline. Repulsion also allows the growth cones of commissural neurons to leave the midline and reach the contralateral side of the CNS, and prevents them from returning to the midline after crossing. Recent studies have shown that repulsive signals are transduced via interactions between the Roundabout (Robo) receptor expressed on neuronal growth cones and the extracellular matrix protein Slit, which is produced by midline glia (Kidd et al., 1999). Slit binds directly to Robo and can mediate repulsion of Robo-expressing growth cones (Brose et al., 1999; Li et al., 1999; Nguyen Ba-Charvet et al., 1999; for review see Zinn and Sun, 1999). In *slit* mutants, all interneuronal axons converge on the midline and remain there, suggesting that repulsion has been eliminated. *robo* mutants, however, have a weaker phenotype in which longitudinal axons cross to the contralateral side of the embryo and then follow looping pathways that traverse the midline multiple times (Seeger et al., 1993; Kidd et al., 1998a,b). The difference between the *robo* and *slit* phenotypes is likely to be due to the existence of a second Robo protein, Robo2, which could mediate repulsion of some growth cones by Slit even when Robo is absent (Kidd et al., 1998a, 1999).

Another component of the repulsive pathway is Commissureless (Comm), a transmembrane protein that is expressed by midline glia and transferred to commissural axons by an unknown mechanism (Tear et al., 1996). Transferred Comm causes downregulation of Robo, neutralizing the repulsive signal and allowing commissural axons to cross. In *comm* loss-of-function mutants, Robo fails to be downregulated, and as a result all axons are repelled from the midline (Seeger et al., 1993; Kidd et al., 1998b).

Here we report the isolation of mutations in the gene encoding the fourth neural RPTPs, DPTP10D. *Ptp10D* single mutants are viable and fertile, and display no abnormal embryonic phenotypes. The phenotypes of mutants that lack both DPTP10D and DPTP69D, however, reveal that RPTPs have important roles in the control of axon guidance across the CNS midline. This had not been apparent before now because a triple mutant that lacks all three of the previously characterized RPTPs has a relatively normal CNS axon array (Desai et al., 1997a; Q. S. and K. Z., unpublished results).

When DPTP10D and DPTP69D are removed, we find that a subset of longitudinal axons are rerouted across the midline. Elimination of all four neural RPTPs converts most longitudinal pathways into commissures, indicating that tyrosine phosphorylation controls the manner in which growth cones respond to midline signals. DPTP10D and DPTP69D genetically interact with Robo, Slit and Comm, and these interactions suggest that the RPTPs are positive regulators of Robo signaling pathways.

MATERIALS AND METHODS

Genetics

The *Ptp10D* gene is contained within three cosmid clones: cos 1, cos 8 and cos F (Fig. 1). *EP1332* (BDGP line EP(X)1172) was isolated by Rorth et al. (1998). A short segment of *EP1332* flanking sequence is available in GenBank (no. AQ025398). The *EP1332* insertion was mapped by Southern DNA hybridization to a 5 kb *Eco*RI fragment of cos 8 that is 5′ to the breakpoint of *Df(1)59* (Bahri et al., 1997). *EP1332* is therefore located about 5 kb upstream of the translation start of DPTP10D. Imprecise excision lines were generated as described by Hamilton and Zinn (1994). Since deletions in the *Ptp10D/bif* region are viable, we were able to screen for deletions by PCR analysis of genomic DNA from single adult flies (Gloor et al., 1993) with primer sets specific to sequence tags at various locations (Fig. 1). The deletion in $Ptp10D^{1}$ starts from the *EP1332* insertion site and ends between primer sets 10D-1 and 10D-2. The P element line *P842* and deletion *Df(1)59* were previously described by Bahri et al. (1997). *Df(1)59* is an approx. 60 kb deletion which removes the entire coding regions of *bif* and *Ptp10D*. *Df(1)101* was generated by mobilizing *P842* and selecting for lines missing the 10D-4 PCR fragment. One of the breakpoints of *Df(1)101* falls within a 14 kb region 3′ to 10D-3. Because this region contains repetitive sequences, we were unable to map the precise location of this breakpoint by Southern hybridization. The other breakpoint of *Df(1)101* is 3′ to the *P842* insertion site. Sequences of primers used for mapping are available on request.

Immunohistochemistry

Whole-mount antibody staining of staged fly embryo collections was performed essentially as described by Patel (1994). Monoclonal antibodies (mAbs) 1D4 (Van Vactor et al., 1993), 3F11 (anti-PTP69D; Desai et al., 1994), 45E10 (anti-PTP10D; Tian et al., 1991), 8C4 (anti-DLAR; B. Burkemper and K. Z., unpublished), and 10D3 (anti-Wrapper (Noordermeer et al., 1998) were used at a dilution of 1:5. BP102 (Seeger et al., 1993) was used at dilution of 1:10. For staining with anti-connectin mAb C1.427, embryos were fixed for 20 minutes in 4% formaldehyde/PEM buffer, and incubated with a 1:3 dilution of the C1.427 supernatant (Meadows et al., 1994). mAb staining was visualized using HRP-conjugated secondary antibodies and DAB immunohistochemistry. Mutant embryos were identified by the absence of staining with particular anti-RPTP mAbs, sorted, and restained with 1D4, BP102 or C1.427. Dissected embryos were photographed on a Zeiss Axioplan microscope using DIC optics.

DiI labeling, neuroblast identification and clonal analysis

We delivered DiI (1,1′-dioctadecyl-3,3,3′,3′-tetramethylindocarbocyanine perchlorate; Molecular Probes, Inc.) to neuroectodermal cells by the method of Bossing and Technau (1994), with modifications described by Schmid et al. (1999). Embryos were labeled at stage 8. After 10 hours at 16°C, embryos developed to stage 11; at this stage, the parasegmental groove, the segmental groove and the midline are used as morphological landmarks for NB identification and GFP-marked balancers are used to distinguish homozygous embryos. By 37 hours after egg laying at 16°C, the embryo is well advanced into stage 17. Dissected stage 17 embryos were imaged on a Biorad 1024 microscope, using a Leitz 50× water immersion lens, as 1.5 μm step *z*-series. Data were collected at 568 nm excitation (for DiI), and each *z*-series was immediately rescanned using Nomarski optics to determine cellular positions within the CNS and identify motoneuronal target muscle(s). Cell and axon measurements were done with Biorad software calibrated to a stage micrometer. Biorad

software was used to project each *z*-series to form 2-dimensional images, which were assembled into figures using Photoshop (v 5.0) and Freehand (v 7.02) software.

RESULTS

Isolation of mutations in the *Ptp10D* gene

To isolate *Ptp10D* mutations, we employed standard P element mutagenesis techniques. Several P element insertions have been mapped to the cytological location 10D. One of these, *EP1332*, is inserted less than 5 kb upstream of the translation start of *Ptp10D* (Fig. 1; see Materials and Methods). Embryos homozygous or hemizygous for *EP1332* express very low levels of DPTP10D protein as assayed by staining with mAbs against DPTP10D (Tian et al., 1991). The phenotypic analysis described below indicates that the *EP1332* insertion is a hypomorphic *Ptp10D* mutation. In order to generate mutations that delete *Ptp10D* coding sequences, we mobilized *EP1332* and isolated five imprecise excision derivatives that delete the first coding exon of *Ptp10D*, which includes the ATG and the DNA encoding the signal sequence. The breakpoints of one of these deletions, $Ptp10D^1$, are indicated in Fig. 1.

Another *P* element in the region, *P842*, was previously described by Bahri et al. (1997). *P842* is inserted 3′ to *bifocal* (*bif*), the gene adjacent to *Ptp10D* (Fig. 1). We carried out similar imprecise excision procedures for *P842* and isolated two deletion lines, *Df(1)59* and *Df(1)101*. *Df(1)59* completely removes the *Ptp10D* and *bif* genes, while *Df(1)101* deletes most of the *Ptp10D* coding sequence (but does not remove the first exon), and all of the *bif* coding sequence (Fig. 1).

$Ptp10D^1$ deletes the ATG and signal sequence, and we were unable to detect any DPTP10D protein in $Ptp10D^1$ embryos. Thus, it is likely to be a null allele. $Ptp10D^1$, *Df(1)59*, *Df(1)101*, and a transheterozygous combination of $Ptp10D^1$ and *Df(1)101* all produce the same phenotypes when combined with *Ptp69D* (see below). $Ptp10D^1$ and *Df(1)101* do not overlap, so the only gene likely to be affected in these transheterozygotes is *Ptp10D*. Finally, the hypomorphic insertion *EP1332* is a *P* element containing multiple binding sites for the yeast transcriptional activator GAL4 (Rorth, 1996), oriented in a manner which would direct GAL4-dependent transcription of *Ptp10D*. When *EP1332* is crossed to *C155-GAL4* (Lin and Goodman, 1994), a fly line in which GAL4 is expressed in all postmitotic neurons, DPTP10D is now also expressed at high levels in neurons. This expression rescues the phenotype conferred by *EP1332* (see below). All of these data indicate that the phenotypes described below are due to the absence of the DPTP10D protein.

Ptp10D Ptp69D double mutant embryos display a synergistic midline crossing phenotype

$Ptp10D^1$, *Df(1)59* and *Df(1)101* are all homozygous viable and fertile, and we were unable to detect any embryonic phenotypes conferred by these mutations. We focused our analysis on the nervous system, since DPTP10D is expressed only on CNS axons in the embryo (Tian et al., 1991; Yang et al., 1991). Fig. 2B shows the CNS of a $Ptp10D^1$ embryo stained with the 1D4 mAb, which recognizes the transmembrane form of Fasciclin II (Van Vactor et al., 1993). In late stage 16 and early stage 17 embryos, 1D4 stains three distinct axon bundles in each longitudinal connective of the

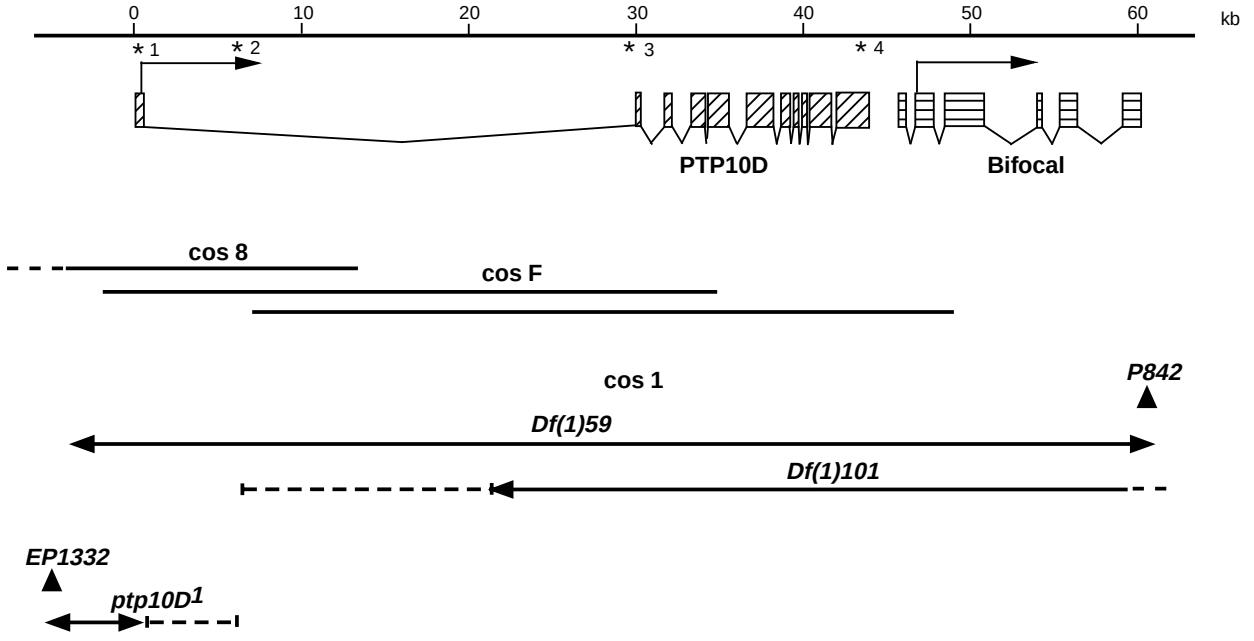

Fig. 1. A molecular map of the *Ptp10D* region. The exons of the *Ptp10D* and *bifocal* genes are indicated by boxes. Arrows above these boxes indicate the direction of transcription. Asterisks indicate the locations of primers used for mapping deletion breakpoints. Three overlapping cosmid clones (cos 1, cos 8 and cos F) that span the *Ptp10D* gene are indicated by lines below the gene map. The insertion sites of two *P* elements (*EP1332* and *P842*) used to generate deletion mutations are indicated by triangles. DNA removed by three deletions generated by imprecise excision of the two P elements, denoted *Df(1)59*, *Df(1)101*, and $Ptp10D^1$, is indicated by lines with arrows. Uncertainties in the deletion break points are indicated by dotted lines. $Ptp10D^1$ removes the entire first exon of *Ptp10D*.

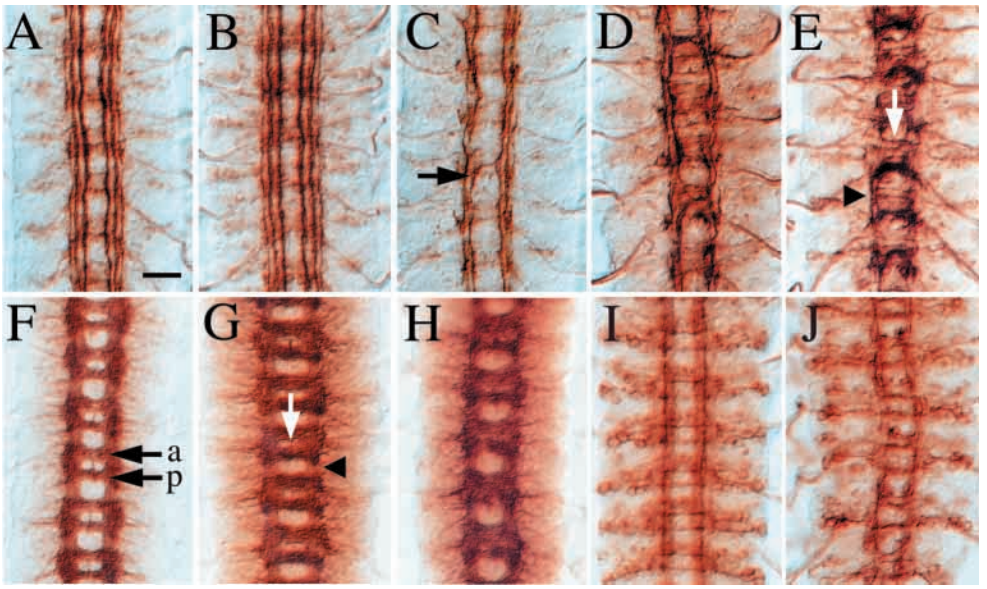

Fig. 2. CNS phenotypes of *Rptp* mutants. Each panel shows a DIC photomicrograph of several segments of the CNS in dissected late stage 16 embryos stained with mAbs 1D4 (A-E), BP102 (F-H) or C1.427 (I,J), using horseradish peroxidase (HRP)-conjugated secondary antibodies and diaminobenzidine (DAB) histochemistry for visualization. (A) Wild type. Note the three distinct axon bundles in each longitudinal connective; the outer bundle is still slightly discontinuous at this stage. There are no commissural bundles stained by 1D4 in late stage 16 embryos, although light cell body staining is visible between the longitudinal tracts in this embryo. (B) *Ptp10D*^{1}. The 1D4 staining pattern of *Ptp10D*^{1} embryos is identical to that observed in wild type. (C) *EP1332*; *Ptp69D*^{1}*/Df(3L)8ex25*. The 1D4-positive axon bundles are fused or interrupted in some segments, and the outer bundle never forms. One axon bundle is misrouted across the midline (arrow). (D) *Ptp10D*^{1}*; Ptp69D*^{1}*/ Df(3L)8ex25*. Multiple axon bundles cross the midline in each segment, and extensive fusion of longitudinal bundles is observed. (E) *Ptp10D*^{1}*; Dlar*$^{13.2}$*/Dlar* $^{5.5}$*; Ptp69D*^{1}*, Df(3R)R3/Df(3L)8ex25, Ptp99A*^{1}. In these quadruple mutant embyros the longitudinal tracts are fragmented (arrowhead), and most 1D4 staining is now on commissural bundles. The bundles that cross the midline do not respect the normal boundaries of the commissures (white arrow). (F) Wild type. In each segment, axons cross the midline within the anterior (a) and posterior (p) commissures (arrows). (G) *Ptp10D*^{1}*; Ptp69D*^{1}*/ Df(3L)8ex25*. The commissures are broader than in wild-type embryos and separated by a smaller space (white arrow). The longitudinal tracts are reduced in the intersegmental regions between the neuromeres (arrowhead). (H) *Ptp10D*^{1}*; Dlar*$^{13.2}$*/Dlar* $^{5.5}$*; Ptp69D*^{1}*, Df(3R)R3/Df(3L)8ex25, Ptp99A*^{1}. Commissures are completely fused in quadruple mutants. (I) Wild type. Two commissural bundles and two longitudinal bundles (one is out of focus) are stained by this mAb. (J) *Ptp10D*^{1}*; Ptp69D*^{1}*/ Df(3L)8ex25*. The commissural bundles are thicker than in wild type, and longitudinal bundles are irregular and sometimes broken. Scale bar, 10 μm.

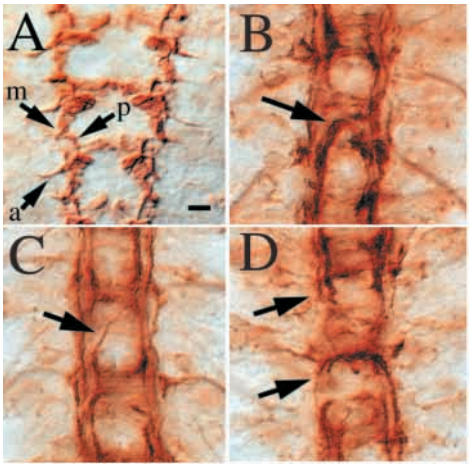

Fig. 3. Axon guidance alterations in *Ptp10D Ptp69D* double mutants. The CNS of late stage 12 (A) and late stage 16 (B-D) *Ptp10D*^{1}*; Ptp69D*^{1}*/ Df(3L)8ex25* embryos, stained with mAb 1D4. (A) Arrows indicate three pioneer growth cones, those of aCC (a), pCC (p) and MP1 (m). The MP1 and pCC axons turn toward the midline in *robo* and *slit* mutants, but they extend normally along ipsilateral longitudinal pathways in *Ptp10D Ptp69D* mutants. (B-D) Examples of guidance alterations observed in stage 16 *Ptp10D Ptp69D* embryos. (B) Rerouting of most of the longitudinal tract across the midline (arrow). (C) Diagonal midline crossing (arrow). (D) Broken longitudinal tracts (arrows). Scale bar, 4 μm.

CNS, but does not stain any commissural bundles. The pattern of 1D4-positive bundles seen in *Ptp10D*^{1} is identical to that observed in wild-type embryos (Fig. 2A; Table 1).

DLAR, DPTP69D, and DPTP99A have partially redundant functions in the control of motor axon guidance (Desai et al., 1996, 1997a; Krueger et al., 1996). A triple mutant lacking all three displays severe motor axon defects, but has a relatively normal pattern of 1D4-positive CNS axons (Desai et al., 1997a; Q. S. and K. Z., unpublished results). This suggests that if these four neural RPTPs are involved in guidance within the CNS, expression of DPTP10D alone is sufficient to compensate for the absence of the other three. DPTP10D is not required when the other three are present, however, since *Ptp10D* mutants have no detectable CNS phenotypes.

To examine whether DPTP10D has a function in CNS axon guidance that is compensated for by another RPTP, we made double mutant combinations in which *Ptp10D* mutations were combined with mutations in each of the other three neural *Rptp* genes. Double mutants lacking DPTP10D and DPTP99A (Hamilton et al., 1995) are viable and exhibit no detectable embryonic phenotypes. *Dlar* mutations are lethal and confer motor axon guidance phenotypes (Krueger et al., 1996; Desai et al., 1997a), but these are unchanged when DPTP10D is also absent. No CNS abnormalities are detectable by 1D4 staining in *Ptp10D Dlar* double mutants (Table 1).

Ptp69D mutations are also lethal and cause motor axon phenotypes (Desai et al., 1996, 1997a). The pattern of 1D4-positive axons in the CNS of *Ptp69D* null mutants is identical to wild type (data not shown). When null *Ptp10D* mutations

(*Ptp10D*[1], *Df(1)59*, and *Df(1)101*) are combined with null mutations in the *Ptp69D* gene (*Ptp69D*[1]*/Df(3L)8ex25* and others; Desai et al., 1997a), a unique and highly penetrant CNS phenotype is observed in double mutant embryos stained with 1D4 (Figs. 2D and 3; Table 1). In these embryos, the longitudinal axon bundles are irregular and often fuse to each

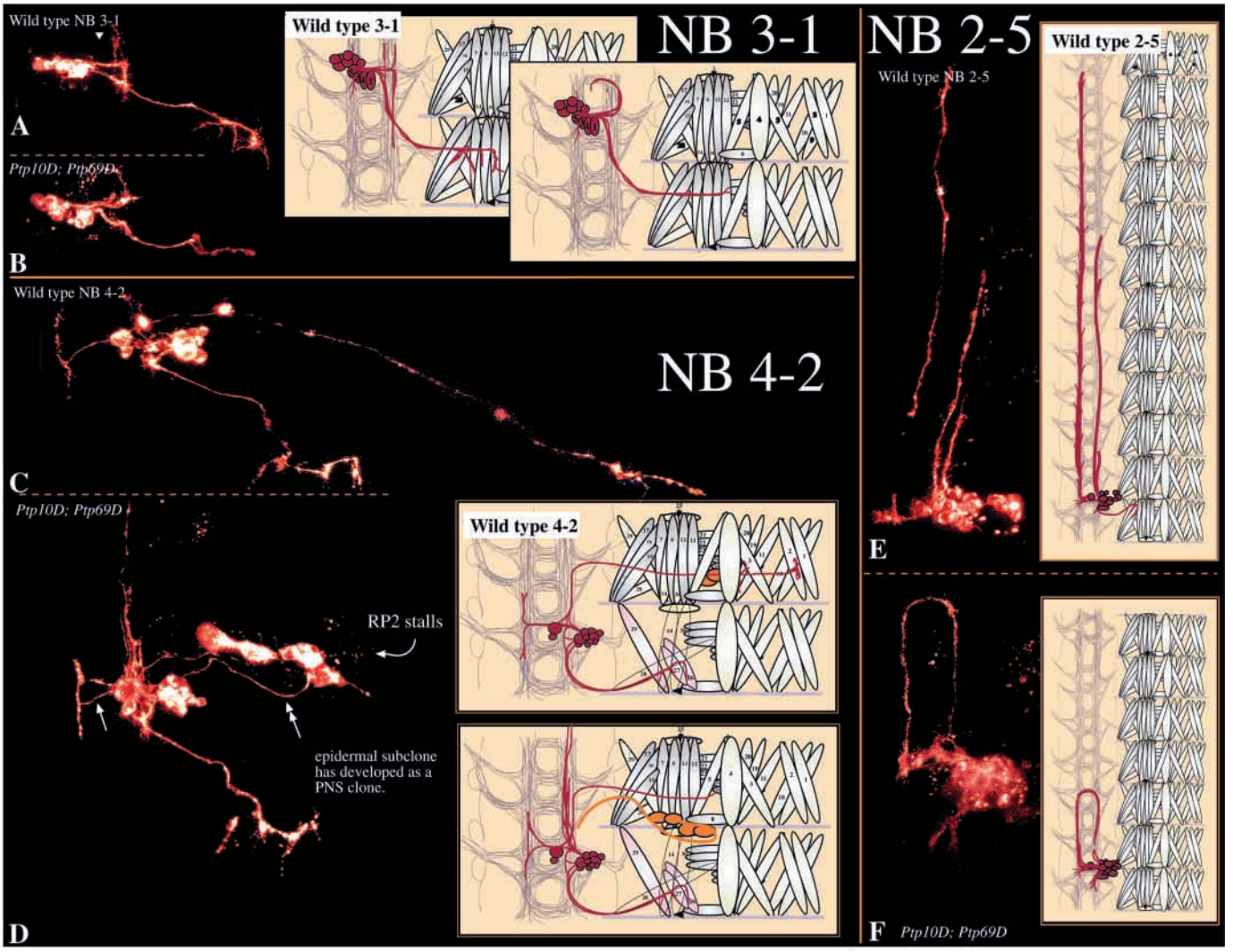

Fig. 4. DiI labeled lineages in wild-type and *Ptp10D Ptp69D* mutant embryos. Neurectodermal cells were labeled with single droplets of DiI at embryonic stage 8 and were examined by confocal microscopy at embryonic stage 17 (Materials and Methods). Each panel consists of a projection of a confocal *z*-series on the left and a diagram of the clone in relation to morphological landmarks on the right. (A) Wild-type 3-1 lineage: RP1,3,4, and 5 motoneurons (MNs) project across the midline to ISNb, forming endings on ventrolateral muscles 6, 7, 12, 13, 14, 28 and 30 (in the abdomen). Interneuronal axons also cross the midline, and fall into two classes: local interneurons project anteriorly in a medial fascicle of the longitudinal connective, and intersegmental interneurons project posteriorly in a more lateral fascicle. (B) In *Ptp10D Ptp69D* double mutants, the RPs form and project to their target muscle fields, but do not form normal endings. Both groups of interneurons fail to segregate into their longitudinal connective pathways and instead circle anteriorly and then back to the midline. (C) Wild-type 4-2 lineage: The RP2 MN projects via the ISN to muscle 2, making side branches at muscles 3 and 19. The CoR MNs constitute the entirety of SNc, sending axons to ventral muscles 26, 27 and 29. There is a cluster of small local interneurons that project across the midline as a tightly fasciculated axon bundle; these neurites project to segmental borders anteriorly and posteriorly. In 25% of 4-2 lineages, an epidermal subclone forms along the RP2 trajectory (yellow cells in diagram). (D) In *Ptp10D Ptp69D* double mutants, RP2 always projects to the ISN, but in 5/6 cases, stalls around muscle 3. The CoRs always form correctly and grow to their appropriate targets, although their synapses have an abnormal appearance. The projection of local interneurons across the midline in the anterior commissure appears wild type, except that the axons always defasciculate into two bundles after crossing the midline (small arrow). Ectopic interneuronal projections form on the ipsilateral side, and project across segmental boundaries in the anterior direction; these axons never form in the wild type. In the lineage shown here, the epidermal subclone developed as a PNS subclone and sent an axon back towards the CNS (double arrow). (E) Wild-type 2-5 lineage: 4-8 intersegmental interneurons send axons anteriorly toward the brain on both the ipsilateral and contralateral sides. The lineage also consists of a MN innervating muscles 15, 16 and 17 via ISNd, local interneurons, a segmental nerve glial cell, and a frequent epidermal subclone. (F) In *Ptp10D Ptp69D* double mutants, contralateral intersegmental interneurons project anteriorly for two segments before crossing the midline and turning back towards the segment of origin. Ipsilateral projections begin to extend anteriorly but do not cross segmental boundaries. The motoneuron fails to exit the CNS via its normal ISNd route.

Table 1. Quantitative analysis of phenotypes

A. Midline crossing of 1D4-positive axons in *Ptp10d Ptp69d* embryos

Genotype	% segments with mAb 1D4-positive commissural bundles	*n**
Ptp10D^{1}	2.6	152
Ptp10D^{1}, *Dlar*$^{5.5}$/*Dlar*$^{13.2}$	1.5	66
Ptp10D^{1}, *Ptp69D*^{1}/*Df(3L)8ex25*	97.4	77
Ptp10D^{1}/*Df(1)101*, *Ptp69D*^{4}/*Df(3L)8ex25*‡	95.5	89

B. Suppression of the *comm* phenotype by removal of DPTP10D and DPTP69D

Genotype	% segments with axons that cross the midline	*n**
comm^{5}	1.4	139
Ptp10D, Ptp69D comm^{5} §	36.8	125

*7-9 segments were scored per dissected late stage 16 embryo.

‡*Ptp69D*^{4}is an unpublished allele that makes no detectable protein. It has a 5′ deletion that does not extend into the *Ptp69D* coding region and does not overlap with *Df(3L)8ex25*.

§The genotypes used were *Ptp10D*^{1}, *Ptp69D*^{1}/*Df(3L)8ex25* and *Df(1)59, Ptp69D*^{1}. These had the same phenotypes with regard to *comm* suppression and have been counted together here. *comm*^{5} is a null allele.

other, so that some segments have only one or two bundles instead of the usual three. The outer 1D4-positive bundle is usually missing or reduced to short, discontinuous stained regions, and breaks in the inner two bundles are also observed. Three or more 1D4-positive bundles that cross the midline are observed within the commissural tracts of each segment. These are never seen in wild-type embryos.

We also examined embryos bearing null *Ptp69D* mutations combined with the hypomorphic *Ptp10D* insertion *EP1332*. DPTP10D protein is normally localized in these embryos, but is present at greatly reduced levels. This combination produces a much weaker phenotype, in which only the outer 1D4 bundle is strongly affected. Occasional fusions of the inner two bundles are also observed, and 1D4-positive bundles cross the commissures in a few segments of each embryo (Fig. 2C). As described above, this double mutant phenotype is rescued by driving high-level DPTP10D expression using a neuronal GAL4 source.

To examine the complete axonal array in double mutant embryos, we used the BP102 mAb, which recognizes an epitope present on all CNS axons (Seeger et al., 1993). Late stage 16 wild-type embryos stained with BP102 display a ladder-like pattern of axons, with two commissural tracts, anterior (A) and posterior (P), in each segment, and bilaterally symmetric longitudinal connectives extending the length of the embryo. At this stage, the longitudinal tracts are thicker than the commissural tracts, especially in the neuropilar region between the anterior and posterior commissures (Fig. 2F). *Ptp10D Ptp69D* double mutant embryos stained with BP102 have broader commissures than wild-type embryos, and the intercommissural space at the midline of the embryo is compressed along the A-P axis (arrow, Fig. 2G). The longitudinal tracts are also somewhat reduced, especially in the intersegmental regions between the neuromeres (arrowhead, Fig. 2G). The 1D4 and BP102 staining patterns are consistent with the hypothesis that some axons that would normally travel within the longitudinal tracts are rerouted across the midline in double mutant embryos.

We also examined double mutant phenotypes using mAb C1.427, which recognizes the Connectin protein (Meadows et al., 1994). In late stage 16 embryos, C1.427 stains two commissural bundles in each segment, two longitudinal bundles, and a small group of neuronal cell bodies (Fig. 2I). In *Ptp10D Ptp69D* double mutant embryos, the C1.427-positive commissural bundles are much thicker, and the longitudinal bundles are irregular and sometimes broken (Fig. 2J).

Although some longitudinal axons cross the commissures in *Ptp10D Ptp69D* double mutant embryos, many others remain within the longitudinal tracts. We wondered whether RPTPs might also be involved in defining these other longitudinal pathways, since all four neural RPTPs are expressed on most or all CNS axons. Accordingly, we constructed and analyzed quadruple mutant embryos bearing null mutations in all four *Rptp* genes. When these embryos were stained with 1D4, a striking phenotype was observed in which most axons cross the midline and all longitudinal pathways are severely disrupted. Only short fragments of longitudinal tracts can be visualized in quadruple mutants (arrowhead, Fig. 2E). Many bundles cross the midline in each segment, and these do not respect the normal boundaries of the commissures (arrows, Fig. 2E). A comparison between Figs 2B and 2E reveals that removing all four RPTPs essentially converts all of the 1D4-positive longitudinal axons into commissural axons.

Quadruple mutants stained with BP102 have fused anterior and posterior commissures, so that a single broad tract crossing the midline is observed in each segment. This phenotype is consistent with the hypothesis that more axons are rerouted across the midline than in double mutants (Fig. 2H). We have also done a phenotypic analysis of all triple mutant combinations, in order to understand how each RPTP contributes to CNS and motor axon guidance, and this will be described elsewhere (Q. S. and K. Z., unpublished results).

Longitudinal pioneer axons develop normally in *Ptp10D Ptp69D* double mutants

1D4-positive axons make a number of different axon guidance errors in *Ptp10D Ptp69D* double mutants. First, the three longitudinal bundles, which are normally separate, fuse with each other for short regions and then separate, and the outer bundle is usually missing (Fig. 2D). Second, the entire 1D4-positive longitudinal tract is sometimes rerouted across the midline within the domain that is demarcated by the anterior and posterior edges of the commissures (Fig. 3B, arrow). The ectopic commissural tract does not appear to avoid the zone between the commissures, which is normally free of axons; this is reflected in the BP102 staining pattern, which shows expansion of the commissures into this zone (Fig. 2G). Third, a longitudinal bundle occasionally wanders diagonally across the midline, traversing the intersegmental region between neuromeres where no axons normally grow (Fig. 3C, arrow). Finally, longitudinal bundles often stop abruptly, causing breaks in the longitudinal tracts (Fig. 3D, arrows).

Although these phenotypes indicate that 1D4-positive axons have been rerouted, they do not show what changes have occurred in the pathways taken by individual growth cones.

This is because many axons are stained by 1D4 in stage 16 embryos, and staining appears to be primarily restricted to established bundles rather than to growth cones. To analyze the behavior of individual growth cones, we examined 1D4-stained double mutant embryos at much earlier stages. During stage 12, the only neurons stained by 1D4 are the longitudinal pioneer neurons MP1, dMP2, vMP2, and pCC, in addition to the motoneuron aCC (Fig. 3A; Seeger et al., 1993). In normal embryos, the vMP2 and pCC axons fasciculate with each other and extend anteriorly, while MP1 and dMP2 axons fasciculate and extend posteriorly. These axons eventually pioneer two continuous longitudinal pathways. One of these is the inner 1D4-positive bundle, and the other is part of the middle bundle (Hidalgo and Brand, 1997).

The pCC, vMP2, MP1, and dMP2 longitudinal pioneer growth cones follow abnormal pathways in *robo* and *slit* mutants, turning toward the midline rather than navigating within the longitudinal tracts (Seeger et al., 1993; Kidd et al., 1998a,b, 1999; Battye et al., 1999). When we examined *Ptp10D Ptp69D* double mutants at stages 12 and 13, however, we found that these growth cones follow normal pathways (Fig. 3A). The longitudinal pathways established by the pioneer axons develop normally up through stage 14. Early C1.427-positive growth cones also follow normal pathways in the double mutants (data not shown). These data suggest that the axons that cross the midline in *Ptp10D Ptp69D* mutants are those of later neurons whose growth cones would normally follow established longitudinal pathways. We have been unable to find antibody or enhancer trap markers that allow selective visualization of these growth cones.

Lineage tracing experiments define growth cone guidance errors made by individual CNS neurons in *Ptp10D Ptp69D* mutants

To visualize individual axons and growth cones that are affected in *Ptp10D Ptp69D* mutants, we performed lineage tracing experiments in which the fluorescent dye DiI was used to label all of the progeny of single neuroblasts (NBs) in vivo. Individual neuroectodermal cells were randomly labeled at stage 8, and the embryos allowed to develop until stage 17, after which DiI-labeled NBs arising from the injected cells were identified based on their positions, and the axons and cell bodies of the NB progeny were visualized by confocal microscopy (Schmid et al., 1999).

Analysis of a large number of NB lineages in the double mutants revealed that many CNS axonal pathways are altered in complex ways by the absence of DPTP10D and DPTP69D. A complete description of these changes will be published elsewhere. Here we describe the projection patterns of three sets of neurons that illustrate essential aspects of the phenotype: the progeny of NBs 3-1, 4-2, and 2-5. No alterations in numbers or positions of cell bodies are observed for these lineages in *Ptp10D Ptp69D* embryos.

The NB 2-5 lineage generates 15-22 cells by stage 17, of which 8-16 are intersegmental interneurons. Some of these (4 to 8 neurons) extend axons across the midline in the anterior commissure; these axons then turn anteriorly in the contralateral longitudinal tract and grow all the way to the brain (up to 10 segments). The remaining intersegmental interneurons (4 to 8 neurons) extend axons anteriorly in the ipsilateral longitudinal tract that stop after projecting about half as far. These contralateral and ipsilateral axons form the most substantial fibers in the longitudinal connectives. There is also a single motoneuron which extends an axon in the ipsilateral ISNd pathway and innervates muscles 15-17 (Schmid et al., 1999; Fig. 4E). In *Ptp10D Ptp69D* mutants (n=3), the contralaterally projecting interneuronal axons cross the midline and turn anteriorly in a normal manner, but then double back across the midline after about two segments and grow posteriorly in the ipsilateral longitudinal tract (Fig. 4F). The axons of the ipsilateral intersegmental neurons grow anteriorly for a short distance and stop. The ISNd motoneuron extends an axon toward the midline that stalls and never enters the ISN root. This lineage illustrates that interneuronal axons abnormally cross the midline in the *Rptp* double mutant, and that a motor axon is deflected toward the midline.

The NB 4-2 lineage produces about 22 cells, including the well-characterized RP2 motoneuron, which extends its axon along the ISN pathway and innervates the dorsal muscle 2. It also generates the CoR motoneurons, whose axons constitute all of the SNc motor nerve. All of the interneurons are local; two or three of them extend axons across the anterior commissure that bifurcate in the contralateral connective (Schmid et al., 1999; Fig. 4C). In *Ptp10D Ptp69D* double mutants (n=6), the RP2 axon stalls before reaching its target, and the CoR axons do not branch onto all of their target muscles. An ipsilateral longitudinal projection is formed that extends anteriorly from the clone and crosses the segment border; this is never observed in wild type. Finally, the local interneuronal projection splits after crossing the midline, so that two pathways form instead of one; this was observed in all lineages examined (Fig. 4D). In summary, this lineage illustrates that abnormal longitudinal pathways are formed in mutant embryos and that pathway selection in the commissures is altered.

NB 3-1 produces the RP1, RP3, RP4 and RP5 motoneurons, which extend axons across the anterior commissure and into the ISNb nerve, eventually innervating the ventrolateral muscles. It also generates a variable number of interneurons, which cross the midline and project both posteriorly (intersegmental interneurons) and anteriorly (local interneurons) in the contralateral connective (Schmid et al., 1999; Fig. 4A). In *Ptp10D Ptp69D* mutants (n=3), the RP neurons extend axons normally across the commissure and into the ISNb nerve, although they do not form normal synapses. The interneuronal projections, however, are radically altered. They still cross the midline, but do not form defined anterior and posterior projections in the contralateral connective. Instead, they grow anteriorly in a circular path around the neuropil, contacting the midline at the end of their trajectory (Fig. 4B). Like the other lineages, 3-1 illustrates that longitudinal pathways cannot form normally. Both the anterior and posterior interneuronal projections are missing, and are replaced by a swirl of axons that grow to the midline. These kinds of pathway alterations could give rise to the connective breaks that are observed in mutant embryos.

Midline cells develop normally in *Ptp10D Ptp69D* mutants

The midline glia that enwrap the commissural tracts express guidance cues for commissural axons such as Netrin and Slit (Harris et al., 1996; Mitchell et al., 1996; Kidd et al., 1999).

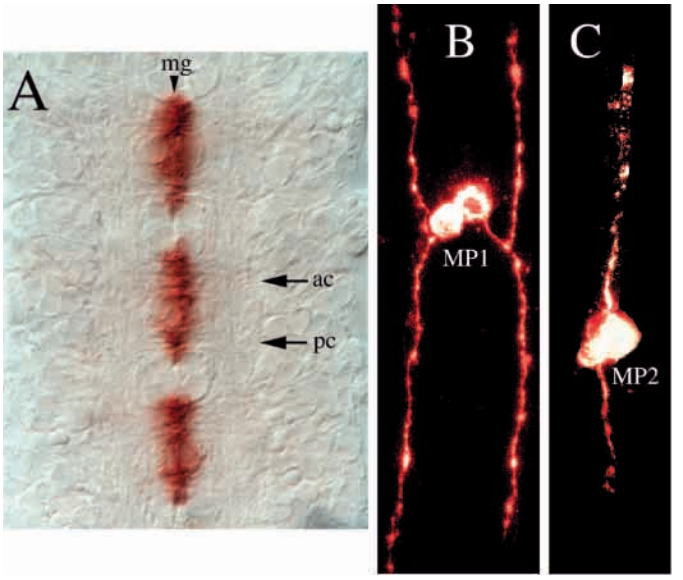

Fig. 5. Midline glia and neurons develop normally in *Ptp10D Ptp69D* mutants. (A) The CNS of a late stage 16 *Ptp10D*^{1}*; Ptp69D*^{1}*/ Df(3L)8ex25* embryo stained with anti-Wrapper mAb to reveal midline glia (mg). The glia enwrap the anterior (ac) and posterior (pc) commissural tracts. The pattern of Wrapper-stained midline glia is indistinguishable from wild type (see Noordermeer et al., 1999; Kidd et al., 1999). (B,C) Midline lineages in *Ptp10D*^{1}*; Ptp69D*^{1}*/ Df(3L)8ex25* embryos, labeled with DiI as in Fig. 4. (B) The MP1 lineage consists of two bilaterally symmetric MP1 neurons, each of which extends anterior and posterior projections. (C) The MP2 'midline' precursor, despite its name, forms bilaterally at the medial edge of the NB columns. It produces the vMP2 neuron, which projects anteriorly, and the dMP2 neuron, which projects posteriorly. Both of these lineages are indistinguishable from wild type (see Bossing and Technau, 1994; Schmid et al., 1999). The MNB lineage is also normal in these mutants. We did not obtain a labeled lineage for the remaining midline precursor, MP3, which produces the two H-cells (Schmid et al., 1999).

To evaluate the origin of the *Ptp10D Ptp69D* phenotype, we wished to determine whether these cells develop normally in mutants lacking these phosphatases. The RPTPs are not expressed in midline glia, but it is possible that their absence from CNS growth cones could indirectly affect the glia by perturbing neuronal-glial interactions. We visualized glia with a mAb recognizing the midline glial surface protein Wrapper (Noordermeer et al., 1998), which is an excellent marker for glial morphology. Fig. 5A shows a *Ptp10D Ptp69D* embryo stained with anti-Wrapper. The midline glial pattern is indistinguishable from that seen in wild type (Noordermeer et al., 1998). Midline glia also appeared normal when stained with an anti-Slit mAb (data not shown).

Midline neurons might also be important for normal navigation of commissural growth cones. We evaluated whether these cells develop normally by dye-filling midline lineages. Fig. 5B,C show MP1 and MP2 lineages in *Ptp10D Ptp69D* mutants. These are also indistinguishable from wild type (Bossing and Technau, 1994; Schmid et al., 1999). Examination of stage 12 embryos with 1D4 (Fig. 3A) also showed that MP1, dMP2 and vMP2 extend axons in a normal manner. Finally, we found that the median neuroblast (MNB) lineage develops normally in these mutants (data not shown).

Ptp10D Ptp69D interacts genetically with *comm*, *robo* and *slit*

The interaction of Robo with Slit produces a repulsive signal that keeps longitudinal axons away from the midline and prevents commissural axons from recrossing. *robo* mutants have a phenotype in which the inner 1D4-positive longitudinal bundle crosses the midline and circles around it. The outer two bundles are less affected (Fig. 6E). Mutations in *slit* confer a more extreme phenotype in which most axons converge on the midline and do not leave (Fig. 7E).

robo is likely to have a weaker phenotype than *slit* because Robo2, a second Slit ligand, can mediate repulsion of some axons when Robo is absent. Consistent with this, removal of one copy of *slit*, which would be expected to reduce repulsion through both Robo family proteins, produces a weak midline crossing phenotype when a copy of *robo* is also removed (*slit/+*, *robo/+*), and enhances the phenotype of *robo* homozygotes (*slit/+*, *robo/robo*) (Kidd et al., 1999). Removing one copy of *slit* in a wild-type background does not produce any abnormal phenotypes.

Another component of this system, the Comm protein, is transferred from midline glia to commissural axons and downregulates Robo, allowing commissural axons to cross the midline (Tear et al., 1996; Kidd et al., 1998b). In *comm* mutants, Robo is not downregulated, and all axons are repelled from the midline. This produces a striking phenotype in which no commissures form (Fig. 6A; Table 1). Because Comm acts through Robo, elimination of Robo suppresses the *comm* phenotype and allows axons to cross the midline; thus, *comm robo* double mutants have phenotypes like those of *robo* single mutants (Seeger et al., 1993).

To investigate the relationship between the Robo/Slit/Comm system and the midline crossing phenotype of the *Rptp* double mutant, we combined the *Ptp10D* and *Ptp69D* mutations with *comm*, *robo* and *slit*. In a *comm Ptp10D Ptp69D* triple mutant, axons are able to cross the commissures. A thick commissural tract, visualized by BP102 (Fig. 6B) or 1D4 (Fig. 6D) staining, is observed in 37% of segments in these triple mutants (Table 1). Note that the 1D4-positive axons would normally not cross the midline even in wild-type embryos. These results suggests that Robo-mediated repulsion from the midline is reduced in the absence of the RPTPs.

When *Ptp10D Ptp69D* is combined with *robo*, a severe phenotype is produced in which most of the 1D4-positive axons converge on the midline (Fig. 6F). Some circles around the midline are still seen in these triple mutants, but many axons fasciculate into a single thick bundle that extends up and down the midline. Vestiges of the lateral longitudinal pathways are also present in some segments. The *robo Ptp10D Ptp69D* phenotype approaches the severity of the *slit* phenotype (Fig. 7E) when visualized with 1D4, suggesting that most repulsion from the midline has been eliminated in these mutants. We also combined *robo* with each of the *Rptp* single mutants, and removed one copy of *robo* from the *Ptp10D Ptp69D* double mutant, but found that none of these combinations produced synergistic phenotypes.

To investigate the relationship between the RPTPs and Slit, we removed one copy of *slit* from the *Ptp10D Ptp69D* double mutant. As shown in Fig. 7, this produces a significant enhancement of the phenotype. More 1D4-positive axons cross the midline, and the longitudinal tracts move closer together,

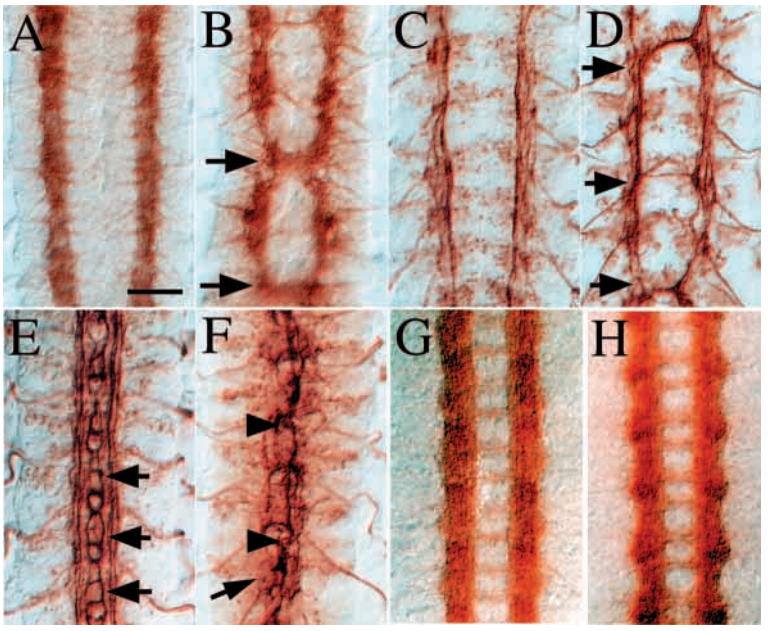

Fig. 6. Genetic interactions between *Ptp10D Ptp69D*, *comm* and *robo*. The CNS in late stage 16 embryos stained with BP102 (A,B), 1D4 (C,F), anti-DLAR mAb 8C4 (G), and anti-DPTP10D mAb 45E10 (H). (A,C) *comm*^{5}. There are no commissural axons in null *comm* mutants (compare to Fig. 2F). (B,D) *Ptp10D*^{1}*; comm*^{5} *Ptp69D*^{1}*/comm*^{5} *Df(3L)8ex25*. Commissural tracts are observed in about every other segment, and some of these are as thick as in wild type (arrows in B). (E) *robo*^{1}. The inner 1D4 bundle circles around the midline (arrows). (F) *Ptp10D*^{1}; *robo*^{1}*/robo*^{1}*; Ptp69D*^{1} *Df(3L)8ex25*. The triple mutant phenotype is much stronger than that of *robo* mutants. Many axons fasciculate into a single thick bundle that extends along the midline (arrowheads). (G,H) Wild-type embryos. (G) DLAR expression. (H) DPTP10D expression. Note that dark staining of the longitudinal tracts is observed for both RPTPs, but the commissural tracts are much less heavily stained (compare to Fig. 2F, which shows even staining of all CNS axons with BP102). This bias is stronger for DLAR than for DPTP10D. Scale bar, 10 μm.

so that the average width of the CNS axonal array decreases from 15.4 μm (±1 μm) in *Ptp10D Ptp69D* to 9.4 μm (±1 μm; 32 segments measured for each genotype) in *Ptp10D Ptp69D, slit*/+ (Fig. 7A,B). The axonal array observed with BP102 is also compressed toward the midline when one copy of *slit* is removed, and more extensive commissural fusion is observed (Fig. 7C,D). These results indicate that, like reducing or eliminating Robo expression, removal of the RPTPs sensitizes the embryo to a 50% reduction in the amount of Slit-mediated repulsion from the midline.

The *Rptp* mutations do not appear to affect Robo or Slit expression, because *Ptp10D Ptp69D* embryos stain in a normal manner with anti-Robo or anti-Slit mAbs (data not shown). Interestingly, however, the expression pattern of two RPTPs in stage 16 embryos may reflect their roles in midline guidance. The Robo protein, although apparently expressed on most or all CNS neurons, is restricted to longitudinal tracts in late embryos due to its downregulation by Comm on commissural axons (Kidd et al., 1998a,b). We found that the DLAR (Fig. 6G) and DPTP10D (Fig. 6H) proteins are also selectively localized to the longitudinal tracts in late stage 16 embryos. This localization, however, is not Comm-dependent, because ectopic expression of Comm on all neurons, which causes Robo to disappear from CNS axons (Kidd et al., 1998b), does not visibly reduce expression of these RPTPs. Ectopic Comm expression also does not affect the other two RPTPs, DPTP69D and DPTP99A, which do not exhibit selective localization to longitudinal tracts (data not shown). It will be of interest to determine the mechanism by which DLAR and DPTP10D become localized to longitudinal axons.

To examine the specificity of the interaction between the *Rptp* mutations and the Robo/Slit/Comm system, we also combined the *Ptp10D Ptp69D* double mutation with a deletion of both Netrin genes. The *Netrin* deletion alone produces a phenotype in which commissures are reduced but not eliminated (Harris et al., 1996; Mitchell et al., 1996), and this phenotype is unaffected when the RPTPs are also removed (data not shown). Thus, the suppression of the *comm* phenotype by the *Rptp* double mutation is due to a selective effect on the repulsion system rather than to a generalized suppression of any phenotype that reduces midline crossing.

We also examined whether the *Rptp* phenotypes are affected by alterations in interaxonal adhesion. In one model, the longitudinal bundle fusion phenotypes could be caused by a decrease in interaxonal adhesion that would allow longitudinal axons to separate from their normal pathways and fasciculate

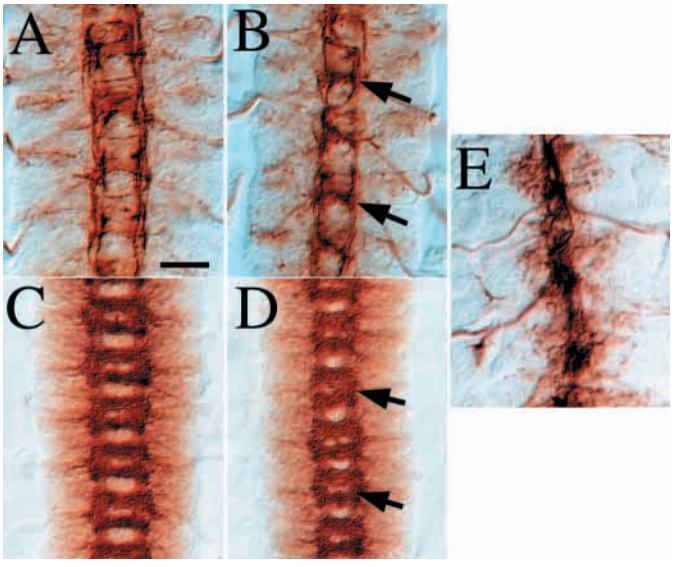

Fig. 7. Genetic interactions between *Ptp10D Ptp69D* and *slit*. The CNS in late stage 16 embryos stained with 1D4 (A,B,E) or BP102 (C,D). (A,C) *Ptp10D*^{1}*; Ptp69D*^{1}*/Df(3L)8ex25*, (B,D) *Ptp10D*^{1}*; slit*^{2}/+; *Ptp69D*^{1}*/Df(3L)8ex25*, (E) *slit*^{1}*/slit*^{2}. The CNS becomes narrower, so that the separation between longitudinal tracts is reduced, when one copy of *slit* is removed from *Ptp10D Ptp69D* (compare B with A, and D with C). Bundles crossing the midline become thicker and more irregular (B, arrows), and commissure fusion is increased (D, arrows). Removal of one copy of *slit* from wild type produces no phenotype. (E) All CNS axons converge on the midline in *slit*^{1}*/slit*^{2} embryos. Scale bar, 10 μm.

with other bundles. Conversely, bundle fusion might be produced by an *increase* in adhesion that would cause two normally separate bundles to adhere to each other. The deviation of longitudinal axons from their normal pathways might also generate midline crossing phenotypes, since it has been shown that ablation of longitudinal pioneer axons causes some follower axons to cross the midline (Hidalgo and Brand, 1997). If this were the case, crossing the midline could be considered to be a 'default' pathway that longitudinal axons select when they fail to adhere normally to their appropriate bundles.

To evaluate these models, we used genetic methods to reduce adhesion within the longitudinal tracts, and determined whether this could enhance or suppress *Ptp10D Ptp69D* phenotypes. In *PlexinA* mutants, which lack a Semaphorin receptor, the outer 1D4 (Fasciclin II)-positive bundle is discontinuous, as it is in *Ptp10D (hypomorph) Ptp69D* mutants. This phenotype is suppressed when one copy of the *FasciclinII (FasII)* gene is removed. Since *FasII* encodes a homophilic adhesion molecule expressed on these axons, this manipulation would be expected to decrease interaxonal adhesion within the 1D4-positive longitudinal bundles (Winberg et al., 1998). To examine whether reducing adhesion in this manner would affect *Rptp* phenotypes, we removed one copy of *FasII* from *Ptp10D Ptp69D* mutants. We observed no effect on their phenotypes, however (data not shown).

DISCUSSION

Four *Drosophila* RPTPs are selectively expressed on CNS axons and growth cones. Genetic analysis of DLAR, DPTP69D and DPTP99A showed that pathfinding by motoneuron and photoreceptor growth cones is dependent on RPTP function (Desai et al., 1996, 1997a; Krueger et al., 1996; Garrity et al., 1999). The signaling mechanisms used by RPTPs to control growth cone guidance are not well understood, although recent studies suggest that DLAR regulates a motor axon pathfinding decision via competitive genetic interactions with the Abl tyrosine kinase (Wills et al., 1999). DLAR also functions in opposition to another RPTP, DPTP99A, at the same growth cone choice point (Desai et al., 1997a). The guidance cues that motoneuron growth cones recognize at such choice points remain unidentified, however, so these results do not define mechanisms by which RPTP activity regulates growth cone navigation in the neuromuscular system.

Here we show that RPTPs regulate growth cone repulsion from the CNS midline. This is a well-characterized decision controlled by identified ligands and receptors. Thus, the finding that RPTPs participate in repulsion should facilitate identification of the components of the signaling pathways in which these phosphatases function.

Although the RPTPs are expressed on most or all interneuronal axons within the CNS, previous genetic studies have not defined CNS phenotypes associated with removal of DLAR, DPTP69D or DPTP99A. In this paper we describe the isolation of mutations in the gene encoding the fourth neural RPTP, DPTP10D, and show that this phosphatase is critical for control of axon guidance at the midline. No embryonic phenotypes are observed in single mutant embryos lacking only DPTP10D. However, when DPTP10D and DPTP69D are both absent, a CNS phenotype is observed in which many longitudinal axons abnormally cross the midline (Figs 2, 3; Table 1).

We visualized ectopic midline crossing in *Ptp10D Ptp69D* double mutants by staining with mAbs 1D4, C1.427 and BP102 (Figs 2, 3), and by dye-filling lineages of neurons derived from specific NBs (Fig. 4). These results indicate that longitudinal pioneer axons are not affected by the *Rptp* mutations (Fig. 3A), but many later axons cross the midline or follow abnormal pathways within the longitudinal tracts. The opposite situation is observed in mutant embryos lacking the Robo receptor, which is expressed on neuronal growth cones and mediates their responses to a midline repulsive signal emanating from the midline glia. Here longitudinal pioneer axons in the medial 1D4-positive longitudinal bundle cross the midline and circle around it, while the later axons in the middle and lateral bundles appear to follow relatively normal pathways (Kidd et al., 1998a,b; Fig. 6E). In triple mutants lacking Robo, DPTP10D and DPTP69D, a very strong phenotype is observed in which all three longitudinal 1D4 bundles are severely affected. In some segments, only a single tract running along the midline is observed (Fig. 6F).

This triple mutant phenotype does not necessarily indicate that Robo and the RPTPs are involved in the same pathways, since simply adding together the guidance errors seen in *robo* and in *Ptp10D Ptp69D* might be expected to generate a phenotype affecting all three 1D4-positive longitudinal bundles. Furthermore, the phosphatases are not required for Robo function in some axons because the growth cones of longitudinal pioneer neurons are rerouted across the midline in *robo* mutants but are not affected in *Ptp10D Ptp69D* embryos (Fig. 3A). We showed that the RPTP mutations do perturb Robo-mediated repulsive signaling at the midline by examining their interactions with two other genes in the repulsive pathway, *comm* and *slit*.

Comm is a protein made by midline glia that is transferred to commissural axons and causes downregulation of Robo. The loss of Robo from these axons allows them to ignore the repulsive signal and cross the midline. When Comm is not expressed, Robo cannot be downregulated and no axons are able to cross (Fig. 6A; Table 1; Tear et al., 1996; Kidd et al., 1998b). Because Comm acts through Robo, in a *comm robo* double mutant the *comm* phenotype is suppressed and extra axons cross the midline (Seeger et al., 1993). We find that *Ptp10D Ptp69D* partially suppresses *comm*, indicating that removal of the RPTPs interferes with reception of the repulsive signal (Fig. 6B,D; Table 1).

The repulsive factor produced by midline glia is likely to be the extracellular matrix protein Slit. In the absence of Slit, all interneuronal axons converge on the midline and remain there (Fig. 7E; Kidd et al., 1999; Battye et al., 1999; for review see Zinn and Sun, 1999). Robo and Slit proteins bind to each other (Brose et al., 1999; Li et al., 1999), and *robo* and *slit* also interact genetically. Removing one copy of *slit*, which produces no phenotype on its own, enhances the *robo* homozgyote phenotype and confers a weak phenotype on *robo*/+ heterozygotes (Kidd et al., 1999). Similarly, the *Ptp10D Ptp69D* phenotype is strengthened by removal of one copy of *slit* (Fig. 7A-D).

Slit ligand is thought to interact with two Robo receptors: Robo and Robo2. Many axons follow normal longitudinal pathways in *robo* mutants, probably because repulsive

signaling through Slit and Robo2 keeps them from converging on the midline. If Robo and Robo2 are the only receptors for Slit, removing both would be expected to eliminate repulsion, producing a *slit*-like phenotype (Kidd et al., 1999). The *robo Ptp10D Ptp69D* triple mutant, when visualized with 1D4, has a phenotype which approaches that of *slit* (Figs 6F, 7E). This suggests that DPTP10D and DPTP69D are required for signaling through Robo2 (or possibly through other, as yet unidentified, Slit receptors). Our data, however, do not support a model in which the RPTPs are *only* involved in Robo2 signaling. If this were the case, one would not expect to observe a genetic interaction between the *Ptp10D Ptp69D* and *robo2* mutations. The *robo2 Ptp10D Ptp69D* triple mutant, however, has a very strong synergistic phenotype, favoring a model in which DPTP10D and DPTP69D function in repulsive signaling through both Robo receptors (Q. S., J. Simpson, T. Kidd, C. S. Goodman, and K. Z., unpublished results).

Although some longitudinal axons follow normal pathways in the absence of DPTP10D and DPTP69D, they apparently still require RPTP function to avoid the midline. In a quadruple mutant embryo lacking all four neural RPTPs, all 1D4-positive longitudinal pathways are converted into commissural pathways (Fig. 2E). Interestingly, however, the quadruple mutant phenotype is quite different from that of *slit*, because these ectopic commissural axons are still able to leave the midline and cross to the contralateral side of the CNS. Thus, growth to the midline and midline crossing are under separate genetic control in ways we do not yet understand.

The fact that longitudinal axons can be changed into commissural axons by elimination of RPTP activity suggests that tyrosine phosphorylation controls the manner in which growth cones respond to midline repulsive signals. This is consistent with the observation that pharmacological inhibition of tyrosine kinase activity in grasshopper embryos causes a *robo*-like phenotype in which the longitudinal axon of the pCC neuron crosses the midline and circles back to the ipsilateral side (Menon and Zinn, 1998). Further evidence that the effects of the inhibitor may actually be due to blockage of Robo signaling is provided by the recent observation that the *Drosophila* pCC axon in *robo* embryos has a unique branched morphology that is identical in appearance to that of the grasshopper pCC in inhibitor-treated embryos (Murray and Whitington; 1999; Menon and Zinn, 1998).

The repulsive response to midline signals is encoded within the Robo cytoplasmic domain, because chimeric receptors in which the extracellular domain of the attractive Netrin receptor is linked to the Robo cytoplasmic domain mediate repulsion rather than attraction (Bashaw and Goodman, 1999). The cytoplasmic domains of fly, nematode and mammalian Robo family proteins (Robos) contain conserved tyrosine-containing PYATT sequence motifs, suggesting that these domains could be direct targets for tyrosine kinases (Kidd et al., 1998a; Zallen et al., 1998). Phosphorylated tyrosine motifs usually function by binding to SH2 and PTB-domain adapter proteins that mediate downstream signaling events. Robo also contains two proline-rich sequences that could interact with SH3-domain adapters. Robo2 has the tyrosine-containing motif, but lacks the proline-rich sequences (Kidd et al., 1998a).

How are Robo signaling pathways regulated by RPTPs? We have no evidence at present that the RPTPs directly alter signaling by the Robo protein. It is possible that the RPTPs and Robo feed into separate pathways that only intersect after several signaling steps. There is, however, a known mechanism for RPTP-mediated positive regulation of tyrosine kinase pathways that suggests how DPTP10D and DPTP69D could facilitate Robo signaling. During T cell receptor (TCR) signal transduction, the RPTP CD45 removes an inhibitory C-terminal phosphate group from the Src-family tyrosine kinase Lck, thereby activating it and allowing it to phosphorylate the ζ chain of the TCR. The phosphorylated ζ chain in turn binds to an SH2-domain containing tyrosine kinase, ZAP-70, which mediates downstream signaling events. CD45 is required for TCR signaling because in its absence Lck is not activated and thus cannot efficiently phosphorylate the ζ chain (reviewed by Weiss and Littman, 1994). [Interestingly, CD45 may also be involved in the termination of the TCR signaling response, since it can dephosphorylate the ζ chain and prevent it from binding to ZAP-70 (Furukawa et al., 1994).]

Another mammalian receptor phosphatase, RPTPα, also dephosphorylates and activates Src-family kinases (Zheng et al., 1992; den Hertog et al., 1993). Fibroblasts derived from RPTPα knockout mice have reduced Src and Fyn activities, suggesting that RPTPα is an in vivo regulator of Src family kinase function (Ponniah et al., 1999; Su et al., 1999).

By analogy to these pathways, DPTP10D and DPTP69D might regulate growth cone repulsion by activating Src-family tyrosine kinase(s) that phosphorylate Robos. This could explain the genetic data, since the loss of RPTP function would be expected to cause a decrease in the extent of Robo phosphorylation.

One might also propose that positive regulation of repulsion by the RPTPs occurs through direct dephosphorylation of Robos, and that dephosphorylated Robos are more active in signaling. This would be unusual, however, since normally it is the phosphorylated form of a signaling motif that binds to downstream adapters.

A variant of the direct interaction model proposes that Robos become phosphorylated on tyrosines after engagement of Slit, and that DPTP10D or DPTP69D are recruited into a Robo/Slit signaling complex by their interactions with the phosphotyrosine motifs. RPTPs might remain bound to these sites for a significant time period, because they often hydrolyze phosphate-tyrosine bonds quite slowly (for example, see Lim et al., 1998). The RPTPs could then function as adapters themselves, binding to downstream signaling proteins and recruiting them into Robo/Slit receptor complexes. Determining which, if any, of these models is correct will require biochemical or genetic identification of in vivo substrates for RPTPs.

We thank the members of the Zinn group for discussions and comments on the manuscript, and Tom Kidd, Julie Simpson, and Corey Goodman for communication of results before publication. This work was supported by a Human Frontiers Science Project grant (RG0122/1997-B) to K. Zinn and W. Chia, and by an NIH RO1 grant to K. Z.

REFERENCES

Bahri, S. M., Yang, X. H. and Chia, W. (1997). The Drosophila Bifocal gene encodes a novel protein which colocalizes with actin and is necessary for photoreceptor morphogenesis. *Mol. Cell Biol.* **17,** 5521-5529.

Battye, R., Stevens, A. and Jacobs, J. R. (1999). Axon repulsion from the

midline of the *Drosophila* CNS requires Slit function. *Development* **126,** 2475-2481.

Bossing, T. and Technau, G. M. (1994). The fate of the CNS midline progenitors in Drosophila as revealed by a new method for single-cell labeling. *Development* **120,** 1895-1906.

Brose, K., Bland, K. S., Wang, K. H., Arnott, D., Henzel, W., Goodman, C. S., Tessier-Lavigne, M. and Kidd, T. (1999). Slit proteins bind Robo receptors and have an evolutionarily conserved role in repulsive axon guidance. *Cell* **96,** 795-806.

den Hertog, J., Pals, C. E. G. M., Peppelenbosch, M. P., Tertoolen, L. G. J., de Laat, S. W. and Kruijer, W. (1993). Receptor protein tyrosine phosphatase α activates pp60$^{c\text{-}src}$ and is involved in neuronal differentiation. *EMBO J.* **12,** 3789-3798.

Desai, C. J., Gindhart Jr., J. G., Goldstein, L. S. B. and Zinn, K. (1996). Receptor tyrosine phosphatases are required for motor axon guidance in the *Drosophila* embryo. *Cell* **84,** 599-609.

Desai, C. J., Krueger, N. X., Saito, H. and Zinn, K. (1997a). Competition and cooperation among receptor tyrosine phosphatases control motoneuron growth cone guidance in *Drosophila*. *Development* **124,** 1941-1952.

Desai, C. J., Popova, E. and Zinn, K. (1994). A *Drosophila* receptor tyrosine phosphatase expressed in the embryonic CNS and larval optic lobes is a member of the set of proteins bearing the 'HRP' carbohydrate epitope. *J. Neurosci.* **14,** 7272-7283.

Desai, C. J., Sun, Q. and Zinn, K. (1997b). Tyrosine phosphorylation and axon guidance: of flies and mice. *Curr. Op. Neur.* **7,** 70-74.

Furukawa, T., Itoh, M., Krueger, N. X., Streuli, M. and Saito, H. (1994). Specific interaction of the CD45 protein-tyrosine phosphatase with tyrosine-phosphorylated CD3 ζ chain. *Proc. Natl. Acad. Sci. USA* **91,** 10928-10932.

Garrity, P. A., Lee, C. H., Salecker, I., Robertson, H. C., Desai, C. J., Zinn, K. and Zipursky, S. L. (1999). Retinal axon target selection in *Drosophila* is regulated by a receptor protein tyrosine phosphatase. *Neuron* **22,** 707-717.

Gloor, G. B., Preston, C. R., Johnson-Schlitz, D. M., Nassif, N. A., Phillis, R. W., Benz, W. K., Robertson, H. M. and Engels, W. R. (1993). Type I repressors of P element mobility. *Genetics* **135,** 81-95.

Goodman, C. S. (1996). Mechanisms and molecules that control growth cone guidance. *Annu. Rev. Neurosci.* **19,** 341-377.

Hamilton, B. A., Ho, A. and Zinn, K. (1995). Targeted mutagenesis and genetic analysis of a *Drosophila* receptor-linked protein tyrosine phosphatase gene. *Roux's Arch. Dev. Biol.* **204,** 187-192.

Hamilton, B. A. and Zinn, K. (1994). From clone to mutant gene. In *Drosophila melanogaster: practical uses in cell and molecular biology*, (ed. E. Fyrberg and L. S. B. Goldstein), pp. 81-94. San Diego, CA.: Academic Press.

Harris, R., Sabatelli, L. M. and Seeger, M. A. (1996). Guidance cues at the *Drosophila* CNS midline: identification and characterization of two *Drosophila* Netrin/UNC-6 homologs. *Neuron* **17,** 217-228.

Hidalgo, A. and Brand, A. H. (1997). Targeted neuronal ablation-the role of pioneer neurons in guidance and fasciculation in the CNS of *Drosophila*. *Development* **124,** 3253-3262.

Kidd, T., Bland, K. S. and Goodman, C. S. (1999). Slit is the midline repellent for the Robo receptor in *Drosophila*. *Cell* **96,** 785-794.

Kidd, T., Brose, K., Mitchell, K. J., Fetter, R. D., Tessier-Lavigne, M., Goodman, C. S. and Tear, G. (1998a). Roundabout controls axon crossing of the CNS midline and defines a novel subfamily of evolutionarily conserved guidance receptors. *Cell* **92,** 205-215.

Kidd, T., Russell, C., Goodman, C. S. and Tear, G. (1998b). Dosage-sensitive and complementary functions of Roundabout and Commissureless control axon crossing of the CNS midline. *Neuron* **20,** 25-33.

Krueger, N. X., Van Vactor, D., Wan, H. I., Gelbart, W. M., Goodman, C. S. and Saito, H. (1996). The transmembrane tyrosine phosphatase DLAR controls motor axon guidance in *Drosophila*. *Cell* **84,** 611-622.

Li, H. S., Chen, J. H., Wu, W., Fagaly, T., Zhou, L., Yuan, W., Dupuis, S., Jiang, Z. H., Nash, W., Gick, C., Ornitz, D. M., Wu, J. Y. and Rao, Y. (1999). Vertebrate Slit, a secreted ligand for the transmembrane protein Roundabout, is a repellent for olfactory bulb axons. *Cell* **96,** 807-818.

Lim, K. L., Kolatkar, P. R., Ng, K. P., Ng, C. H. and Pallen, C. J. (1998). Interconversion of the kinetic identities of the tandem catalytic domains of receptor-like protein-tyrosine phosphatase PTPalpha by two point mutations is synergistic and substrate-dependent. *J. Biol. Chem.* **273,** 28986-28993.

Lin, D. M. and Goodman, C. S. (1994). Ectopic and increased expression of fasciclin II alters motoneuron growth cone guidance. *Neuron* **13,** 507-523.

Meadows, L. A., Gell, D., Broadie, K., Gould, A. P. and White, R. A. (1994). The cell adhesion molecule, Connectin, and the development of the *Drosophila* neuromuscular system. *J. Cell Sci.* **107,** 321-328.

Menon, K. P. and Zinn, K. (1998). Tyrosine kinase inhibition produces specific alterations in axon guidance in the grasshopper embryo. *Development* **125,** 4121-4131.

Mitchell, K. J., Doyle, J. L., Serafini, T., Kennedy, T. E., Tessier-Lavigne, M., Goodman, C. S. and Dickson, B. J. (1996). Genetic analysis of *Netrin* genes in *Drosophila*-Netrins guide CNS commissural axons and peripheral motor axons. *Neuron* **17,** 203-215.

Murray, M. J. and Whitington, P. M. (1999). Effects of *roundabout* on growth cone dynamics, filopodial length, and growth cone morphology at the midline and throughout the neuropile. *J. Neurosci.* **19,** 7901-7912.

Nguyen Ba-Charvet, K. T., Brose, K., Marillat, V., Kidd, T., Goodman, C. S., Tessier-Lavigne, M., Sotelo, C. and Chedotal, A. (1999). Slit-mediated chemorepulsion and collapse of developing forebrain axons. *Neuron* **22,** 463-473.

Noordermeer, J. N., Kopczynski, C. C., Fetter, R. D., Bland, K. S., Chen, W.-Y. and Goodman, C. S. (1998). Wrapper, a novel Member of the Ig superfamily, is expressed by midline glia and is required for them to ensheath commissural axons in *Drosophila*. *Neuron* **21,** 991-1001.

Patel, N. H. (1994). Imaging neuronal subsets and other cell types in whole-mount *Drosophila* embryos and larvae using antibody probes. In *Drosophila melanogaster: practical uses in cell and molecular biology*, (ed. E. Fyrberg and L. S. B. Goldstein), pp. 446-488. San Diego, CA.: Academic Press.

Ponniah, S., Wang, D. Z. M., Lim, K. L. and Pallen, C. J. (1999). Targeted disruption of the tyrosine phosphatase PTPα leads to constitutive downregulation of the kinases Src and Fyn. *Curr. Biol.* **9,** 535-538.

Rorth, P. (1996). A modular misexpression screen in *Drosophila* detecting tissue-specific phenotypes. *Proc. Natl. Acad. Sci. USA* **93,** 12418-12422.

Rorth, P., Szabo, K., Bailey, A., Laverty, T., Rehm, J., Rubin, G. M., Weigmann, K., Milan, M., Benes, V., Ansorge, W. and Cohen, S. M. (1998). Systematic gain-of-function genetics in *Drosophila*. *Development* **125,** 1049-1057.

Schmid, A., Chiba, A. and Doe, C. Q. (1999). Clonal analysis of *Drosophila* embryonic neuroblasts: neural cell types, axon projections, and muscle targets. *Development* **126,** 4653-4689.

Seeger, M., Tear, G., Ferres-Marco, D. and Goodman, C. S. (1993). Mutations affecting growth cone guidance in *Drosophila*: genes necessary for guidance toward or away from the midline. *Neuron* **10,** 409-426.

Stoker, A. and Dutta, R. B., 463-472. (1998). Protein tyrosine phosphatases and neural development. *Bioessays* **20,** 463-472.

Su, J., Muranjan, M. and Sap, J. (1999). Receptor protein tyrosine phosphatase α activates Src family kinases and controls integrin-mediated response in fibroblasts. *Curr. Biol.* **10,** 505-511.

Tear, G., Harris, R., Sutaria, S., Kilomanski, K., Goodman, C. S. and Seeger, M. A. (1996). Commissureless controls growth cone guidance across the CNS midline in *Drosophila* and encodes a novel membrane protein. *Neuron* **16,** 501-514.

Tian, S.-S., Tsoulfas, P. and Zinn, K. (1991). Three receptor-linked protein-tyrosine phosphatases are selectively expressed on central nervous system axons in the *Drosophila* embryo. *Cell* **67,** 675-685.

Van Vactor, D., Sink, H., Fambrough, D., Tsoo, R. and Goodman, C. S. (1993). Genes that control neuromuscular specificity in *Drosophila*. *Cell* **73,** 1137-1153.

Weiss, A. and Littman, D. R. (1994). Signal transduction by lymphocyte antigen receptors. *Cell* **76,** 263-274.

Wills, Z., Bateman, J., Korey, C. A., Comer, A. and Van Vactor, D. (1999). The tyrosine kinase Abl and its substrate Enabled collaborate with the receptor phosphatase Dlar to control motor axon guidance. *Neuron* **22,** 301-312.

Winberg, M. L., Noordermeer, J. N., Tamagnone, L., Comoglio, P. M., Spriggs, M. K., Tessier-Lavigne, M. and Goodman, C. S. (1998). Plexin A is a neuronal Semaphorin receptor that controls axon guidance. *Cell* **95,** 903-916.

Yang, X., Seow, K. T., Bahri, S. M., Oon, S. H. and Chia, W. (1991). Two Drosophila receptor-like tyrosine phosphatase genes are expressed in a subset of developing axons and pioneer neurons in the embryonic CNS. *Cell* **67,** 661-673.

Zallen, J. A., Yi, B. A. and Bargmann, C. I. (1998). The conserved immunoglobulin superfamily member SAX-3/Robo directs multiple aspects of axon guidance in C. elegans. *Cell* **92,** 217-227.

Zheng, X. M., Wang, Y. and Pallen, C. J. (1992). Cell transformation and activation of pp60$^{c\text{-}src}$ by overexpression of a protein tyrosine phosphatase. *Nature* **359,** 336-339.

Zinn, K. and Sun, Q. (1999). Slit branches out: a secreted protein mediates both attractive and repulsive axon guidance. *Cell* **97,** 1-4.